Contents lists available at ScienceDirect

Chemical Engineering Research and Design

journal homepage: www.elsevier.com/locate/cherd

Design and optimization of CO_2 hydrogenation multibed reactors

*Manuel F. Torcida, Diego Curto, Mariano Martín**

Department of Chemical Engineering, University of Salamanca, Plz. Caídos 1-5, 37008 Salamanca, Spain

ARTICLE INFO

Article history:
Received 22 November 2021
Received in revised form 14 February 2022
Accepted 2 March 2022
Available online 17 March 2022

Keywords:
Biogas
Biomethane
Methanol
CO_2 hydrogenation
Reactor design

ABSTRACT

The use of CO_2 towards the production of chemicals can help in the decarbonization of industry, but the transformation of such a stable compound is a challenge. This work uses genetic algorithms for the design of multi bed reactors for the hydrogenation of CO_2 towards handy products. Two cases of study were evaluated. The production of biomethane from biogas, where the presence of methane in the feedstock represents an additional challenge to achieve a high conversion, and the production of methanol. The optimization addressed the design, bed sizing and number of beds, and the operating conditions of the feedstock, composition, and temperature profile. The optimal configuration of the biomethanation reactor consists of 2 beds using a H_2 to CO_2 ratio of 2.75, operating at 15 atm, limiting the ΔT at each bed to 100 K. A lower number of beds is required if a larger ΔT_{max} is allowed, improving the reactor conversion. The methanol production reactor is recommended to consist of 6 beds operating at 50 atm, with a feed ratio H_2 to CO_2 of 3.5, requiring less catalyst than at higher pressure.

1. Introduction

Waste generation in the form of organic residues and gaseous emissions such as CO_2 are some of the more important concerns of our society (WEC, 2016). The concept of circular economy has provided a strategy towards the valorisation of waste by producing energy, fuels, and chemicals (Korhonen et al., 2018). CO_2 is generated in power plants, concrete facilities as well as in biomass gasification into chemical and fuels. It is a very stable chemical whose further use to produce chemicals (Uebbing et al., 2020) has been presented as an opportunity within the carbon capture and utilization paradigm (Cuéllar-Franca and Azapagic, 2015). In addition, following the circular economy trend, anaerobic digestion has been deemed as a major technology to process organic waste (Gunaseelan, 1997), generating a digestate rich in nutrients that can be further recovered for its use as fertilizers (Martín et al., 2018), and biogas, a mixture consisting mainly of methane and CO_2. The volume of waste produced can allow the substitution of the natural gas by that obtained from biogas in many regions. Despite the large investment required to build the processing facilities (Taifouris and Martín, 2018), as long as biogas is upgraded to natural gas composition, the shipping infrastructure is already available. Therefore, biogas is not only a source of methane, but also of CO_2 that is an additional carbon source to produce chemicals (Hernández and Martín, 2016), in particular methane (Davis and Martín, 2014a) or methanol (Kiss et al., 2016). The target of net zero CO_2 emissions can be achievable by reusing it. Recent studies show that it can become competitive to produce chemicals and fuels from CO_2 hydrogenation if the wind farm (de la Cruz and Martin, 2016) and/or the solar field are installed in regions with high renewable resource (Davis and Martín, 2014b).

The core stage in the transformation of biogas into biomethane, as well as in the production of methanol from CO_2, is its hydrogenation towards each of the products. Even though the methanation of the CO_2 within the biogas can be carried out within the digester, as it has been presented in the literature (Tynjala, 2015) and demonstrated at small scale (Witte et al., 2010), the catalytic hydrogenation of CO_2 is preferred. This alternative has already been tested at the level of proof of concept (Kirchbacher et al., 2016), and it is similar to the production of methanol in industry nowadays (Martín, 2016a). In the case of the methanation of biogas, the presence of methane already in the feedstock affects the yield and operation of a reaction that is governed by chemical equilibrium. Recently, some experimental studies have presented hydrogenation as a biogas upgrading alternative instead of capturing and removing the CO_2 from the mixture (Stangeland et al., 2017). According to this last work, further catalyst development is

* *Corresponding author.*
E-mail address: mariano.m3@usal.es (M. Martín).
https://doi.org/10.1016/j.cherd.2022.03.007

Nomenclature

a	Hydrogen feed ratio
A	Area (m^2)
b	Feed ratio
C_i	Cost (€/kg) of species i
Cat	Catalyst cost (€)
Cp	Heat capacity (kJ/kg K)
d	Feed ratio
D_c	Vessel internal diameter (m)
D_p	Particle diameter (m)
e	Thickness (in)
EC_{Annual}	Equipment cost annualized (€/yr)
F_i	Molar flow rate of component i (kmol/s)
G	Mass flow
HX	Heat Exchanger
k_i	Kinetic constant
K_{p1}	Equilibrium constant
Ki	Adsorption constant of species i
L	Vessel Length (m)
P	Total pressure (atm/kPa)
P_i	Partial pressure of species i (kPa)
p_i	Partial pressure of species i (bar)
r_i	Reaction rate of species i
R	Vessel radius (m)
S	Material tension (psi)
T	Temperature (K) unless otherwise specified
U	Global heat transfer coefficient (W/m^2 ºC)
W	Electrical energy (kW)
W_i	Weight of element i (kg)
z	Polytropic coefficient
Z	Objective function (€/s)

Symbols

β	Center's constants
η	reaction efficiency
θ	Surface coverage
ΔH_f	Formation enthalpy (kJ/kg)
ε	Porosity
μ	Viscosity
ρ	Density
ρ_b	bed density
ϕ_σ	Shape factor (Ergun equation)
ϕ	Total amount of oxidised centres

Subindex

Annual	Annualized variable
Prod	Products
Wa	Water
Steel	Steel

required, but the evaluation of various reactors is already in progress (Schidhauer and Biollaz, 2015). The literature is rich in studies evaluating the hydrogenation of CO_2. To produce biomethane, its kinetics (Bader et al., 2011; Falbo et al., 2018), thermodynamics (Sahebdelfar and Ravanchi, 2015), one bed reactor modelling (Materazzi et al., 2017), including industrial scale operation (Dannesboe et al., 2020), and the analysis of the operation (Schidhauer and Biollaz, 2015) have been evaluated. The work on the production of methanol from the hydrogenation of CO_2 is also extensive in the literature, performing sensitivity studies of the operating conditions considering one single bed (Kiss et al., 2016; Milani et al., 2015), comparing different kinetic models (Meyer et al., 2016), considering the use of renewable resources (Seidel et al., 2018), and modelling the reactor considering one single catalytic bed (Rafiee, 2020). Similarly, the analysis of the entire processes for the hydrogenation of CO_2 towards biomethane and methanol has also been carried out to evaluate the economics. The production of biomethane has been addressed using a simulation approach to produce biomethane from biosyngas (Gassner and Marechal, 2009), or a mathematical optimization one to evaluate the methanation of CO_2 using renewable hydrogen (Gassner and Marechal, 2009). The methanol production process has also been studied and analyzed from different perspectives, including simulation and optimization-based approaches. The simulation approach uses ASPEN as platform, evaluating the CO_2 capture from a coal power plant (Van-Dal and Bouallou, 2013), and comparing different configurations of the process, either direct hydrogenation or the reduction of CO_2 to CO and the hydrogenation of the CO in a second stage (Anicic et al., 2014). A more detailed kinetics is also included in the work by Kiss et al. (2016). The optimization-based line of work follows either a simulation-based procedure or a mathematical optimization approach. The first of the two is used in several works, presenting a sensitivity analysis of the process using CHEMCAD to perform a techno-economic analysis, evaluating the effect of the raw material prices (Pérez-Fortes et al., 2016), as well as the use a surface of response surrogate model to optimize the performance of the process (Borisut and Nuchitprasittichai, 2019). Alternatively, the mathematical based one evaluates the variability of renewable resources presenting a two-stage approach to include uncertainty in process design (Martin, 2016b).

However, the analysis of such reactors has been limited to the design of the particles (Zimmermann et al., 2020), the evaluation of the safety operation (Fache et al., 2018), kinetic studies (Kiss et al., 2016; Milani et al., 2015) or the optimization of the pellet layers (Hwang and Smith, 2008; Schaaf et al., 2014). The simultaneous design of multibed units and the optimization of the operating conditions with detailed kinetics, has not been addressed. These units consist of a discrete number of beds due to the heat transfer limitations and the high exothermic reactions involved. The complex kinetics poses an additional challenge for the analysis, design, and optimization. Only for the case of ammonia, the reactor characteristics were optimized in a two-stage approach, but the number and features of the beds used in the reactor were not optimized (Sánchez and Martín, 2018). Current projects on CO_2 methanation are discussed in a recent review (Rönsch et al., 2016).

In this work genetic algorithms are used for the design and selection of the optimal operating conditions of multibed reactors for the use of CO_2 to produce fuels and chemicals. Two cases of study are evaluated, the production of biomethane via biogas methanation and the production of methanol from CO_2 hydrogenation. The number of beds, the bed length and the operating conditions are variables towards an optimal design of such units. The rest of the paper is structured as follows. Section 2 shows the details of the modelling of the reactors. Section 3 presents the results of the features and the operation of the reactors. Finally, some remarks are presented in section 4.

2. Reactor modelling

This section is divided to present the modelling features of each of the two cases under evaluation, the methanation reactor using biogas as raw material and the production of methanol from CO_2 hydrogenation. The reactors are multi-bed ones with intercooling. The model for a bed is described in this section. After that, the gas is cooled down to the inlet temperature and fed to another bed. The cooldown step is carried out in an external heat exchanger using water as cooling agent. The number of beds and the operating conditions including feed pressures and temperatures to the beds and the feed composition will be determined in the optimization. The models are presented using the original units from the references. However, the results on the paper are homogenized. The kinetic models were experimentally validated at the source, see cited

references, and are assumed to be valid within the range of operation.

2.1. Single bed model for the methanation stage

The methanation stage is a mature technology that has been studied over the years (Davies and Lihou, 1971). However, the main challenge in the methanation of biogas is the presence of a large amount of methane in the purified biogas stream, which determines the need for an excess of hydrogen and the selection of the proper lengths and number of beds to drive the equilibrium to products. The high cost of renewable hydrogen defines this section. Two main reactions govern the methanation of CO_2, the methanation itself, eq. (1), and the reverse water gas shift reaction, eq. (2). eq. (3) describes the hydrogenation of the CO_2 but is linearly dependent of the other two.

$$CO+3H \rightleftarrows CH_4 + H_2O \tag{1}$$

$$CO_{2(g)} + H_{2(g)} \rightleftarrows CO + H_2O_{(g)} \tag{2}$$

$$CO_2+4H_2 \rightleftarrows CH_4+2H_2O \tag{3}$$

The kinetics of each reaction is given as follows, eq. (4), in kmol/kg $_{cat}$ · h (Xu and Froment, 1989).

$$\begin{aligned} r_I &= \frac{k_1}{P_{H_2}^{2.5}}\left(P_{CH_4}\cdot P_{H_2O} - \frac{P_{H_2}^3 \cdot P_{CO}}{K_1}\right)\frac{1}{DEN^2} \\ r_{II} &= \frac{k_2}{P_{H_2}}\left(P_{CO}\cdot P_{H_2O} - \frac{P_{H_2}\cdot P_{CO_2}}{K_2}\right)\frac{1}{DEN^2} \\ r_{III} &= \frac{k_3}{P_{H_2}^{3.5}}\left(P_{CH_4}\cdot P_{H_2O}^2 - \frac{P_{H_2}^4 \cdot P_{CO_2}}{K_1\cdot K_2}\right)\frac{1}{DEN^2} \end{aligned} \tag{4}$$

Where variable DEN is defined by eq. (5) as a function of adsorption constants, K_i, and the partial pressures, P_i, of the different species:

$$DEN = 1 + K_{CO}\cdot P_{CO} + K_{H_2}\cdot P_{H_2} + K_{CH_4}\cdot P_{CH_4} + \frac{K_{H_2O}\cdot P_{H_2O}}{P_{H_2}} \tag{5}$$

The kinetic constants, k_i, are given by eq. (6) for each of the reactions:

$$\begin{aligned} k_1 &= 9.490\cdot 10^{16} e^{\left(-\frac{28879}{T}\right)} [=] \frac{kmol\cdot kPa^{0.5}}{kg\cdot h} \\ k_2 &= 4.390\cdot 10^{4} e^{\left(-\frac{8074.3}{T}\right)} [=] \frac{kmol\cdot kPa^{-1}}{kg\cdot h} \\ k_3 &= 2.290\cdot 10^{16} e^{\left(-\frac{29336}{T}\right)} [=] \frac{kmol\cdot kPa^{0.5}}{kg\cdot h} \end{aligned} \tag{6}$$

and the adsorption constants, K_j, for each component j, are as follows, eq. (7):

$$\begin{aligned} K_{CH_4} &= 6.65\cdot 10^{-6} e^{\left(\frac{4604.28}{T}\right)} [=] kPa^{-1} \\ K_{H_2O} &= 1.77\cdot 10^{3} e^{\left(-\frac{10666.35}{T}\right)} [=] kPa^{-1} \\ K_{H_2} &= 6.12\cdot 10^{-11} e^{\left(\frac{9971.13}{T}\right)} [=] kPa^{-1} \\ K_{CO} &= 8.23\cdot 10^{-7} e^{\left(\frac{8497.71}{T}\right)} [=] kPa^{-1} \end{aligned} \tag{7}$$

Finally, the equilibrium constants, Ki, can be computed using the following expressions (Davies and Lihou, 1971):

$$\begin{aligned} K_1 &= 10266.76 e^{\left(-\frac{26830}{T} + 30.11\right)} [=] kPa^2 \\ K_2 &= e^{\left(\frac{4400}{T} - 4.063\right)} \\ K_3 &= K_1\cdot K_2 [=] kPa^2 \end{aligned} \tag{8}$$

The partial pressures of each of the species are computed from the molar flows as in eq. (9):

$$P_i = \frac{F_i}{\sum_i F_i}\cdot P_T \tag{9}$$

The reaction does not go as far as the equilibrium, and the efficiency is a function of the length of the bed. The effectivity factors are defined by eq. (10):

$$\eta_i = \frac{r_{actual}}{r_{atsurface}} \tag{10}$$

Where empirical correlations were developed for each of the reference species as follows Vara (2000), eq. (11)

$$\begin{aligned} \eta_{CH_4} &= a_1 + b_1 Z + c_1 Z^2 + d_1 Z^3 + e_1 Z^4 + f_1 Z^5 \\ \eta_{CO_2} &= a_2 + b_2 Z + c_2 Z^2 + d_2 Z^3 + e_2 Z^4 + f_2 Z^5 \end{aligned} \tag{11}$$

Table 1 shows the coefficients of eq. (11).

Thus, the kinetics for all the species can be written as eq. (12)

$$\begin{aligned} \frac{dF_{CO_2}}{dz} &= r_{CO_2} = \rho_{bed}\cdot A_{cross}\cdot (r_{II} + r_{III})\cdot \eta_{CO_2} \\ \frac{dF_{H_2}}{dz} &= r_{H_2} = \rho_{bed}\cdot A_{cross}\cdot (3\cdot r_I + r_{II} + 4r_{III})\cdot \eta_{CO_2} \\ \frac{dF_{CO}}{dz} &= r_{CO} = \rho_{bed}\cdot A_{cross}\cdot (r_I - r_{III})\cdot \eta_{CO_2} \\ \frac{dF_{H_2O}}{dz} &= r_{H_2O} = -\rho_{bed}\cdot A_{cross}\cdot (r_I + r_{II} + 2r_{III})\cdot \eta_{CH_4} \\ \frac{dF_{CH_4}}{dz} &= r_{CH_4} = -\rho_{bed}\cdot A_{cross}\cdot (r_I + r_{III})\cdot \eta_{CH_4} \end{aligned} \tag{12}$$

Table 1 – Coefficients for kinetic rate efficiency.

η_{CH4}						
Z (m)	a1	b1	c1	d1	e1	f1
0–0.2	$3.40271\cdot10^{-02}$	$1.50706\cdot10^{-01}$	$-1.43056\cdot10^{-01}$	$8.95366\cdot10^{-01}$	−3.91470	6.22014
0.2–2	$3.46465\cdot10^{-02}$	$2.78045\cdot10^{-03}$	$-5.60737\cdot10^{-03}$	$4.59855\cdot10^{-03}$	$-1.80038\cdot10^{-03}$	$2.73842\cdot10^{-04}$
2–12	$3.53026\cdot10^{-02}$	$-5.63342\cdot10^{-04}$	$1.04288\cdot10^{-04}$	$-1.07611\cdot10^{-05}$	$5.56779\cdot10^{-07}$	$-1.10707\cdot10^{-08}$
η_{CO2}						
Z (m)	a1	b1	c1	d1	e1	f1
0–0.2	$3.41762\cdot10^{-02}$	$1.91920\cdot10^{-02}$	$-2.71999\cdot10^{-01}$	2.16797	−8.65165	1.35279
0.2–2	$3.46135\cdot10^{-02}$	$2.58231\cdot10^{-03}$	$4.80816\cdot10^{-03}$	$3.77979\cdot10^{-03}$	$-1.43009\cdot10^{-03}$	$2.11362\cdot10^{-04}$
2–11	$3.53703\cdot10^{-02}$	$-5.80316\cdot10^{-04}$	$1.53452\cdot10^{-04}$	$-2.36097\cdot10^{-05}$	$1.85678\cdot10^{-06}$	$-5.62914\cdot10^{-08}$

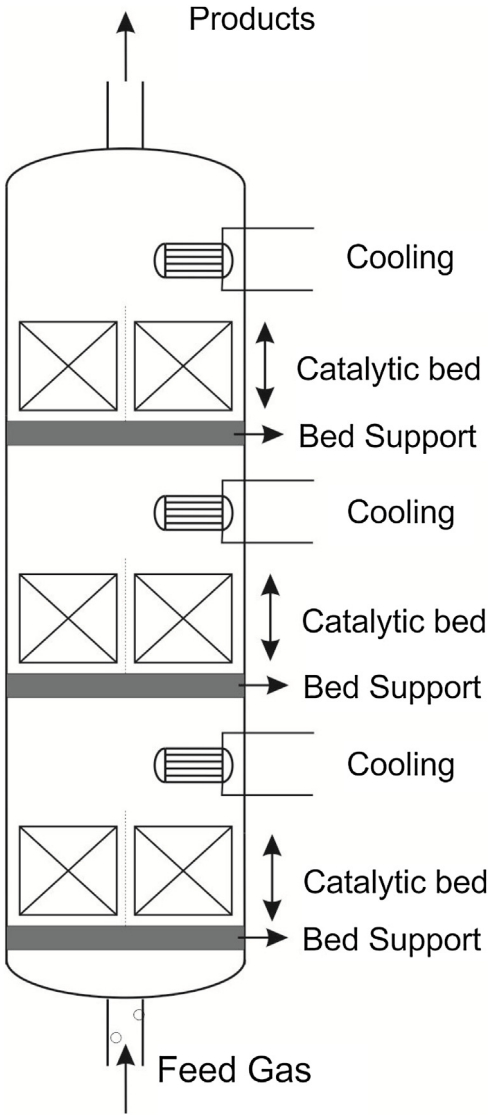

Fig. 1 – Scheme of the methanation reactor.

The energy balance is formulated as eq. (13):

$$\frac{dT}{dz} = \frac{\sum_i (-r_i)\left[\Delta H_{R,i}(T_R) + \int_{T_R}^{T} \Delta C p dT\right]}{F_{Ao}\left(\sum_{i=1}^{n} \Theta_i C p_i + x\Delta C p\right)} \quad (13)$$

And the pressure drop is computed following Ergun's equation, eq. (14):

$$\frac{dP}{dz} = -\frac{G(1-\varepsilon)}{\rho_o D_p \varepsilon^3}\left[\frac{150(1-\varepsilon)\mu}{D_p} + 1.752G\right]\frac{P_o}{P}\frac{T}{T_o}\frac{F_T}{F_{To}}$$
$$G = \frac{\sum_i F_{io} M_i}{A_c} \quad (14)$$
$$A_c = \pi D^2 4$$
$$W = \rho_b A_c z$$
$$\mu \approx cte$$

The catalytic bed is made of Haldor TopsØe Ni/Mg Al_2O_4 Spinel with a particle diameter of 0.025 m, a particle density of 2355.2 kg/m^3, a bed density of 1507.3 kg/m^3, and a porosity (ε) of 0.368. It typically operates around 580 K and a pressure of 15 atm. Fig. 1 shows the scheme of a multibed reactor for the methanation of biogas.

2.2. *Single bed model for the production of methanol*

In the reactor three typical reactions take place simultaneously, the hydrogenation of the CO_2 to methanol, the hydrogenation of CO and the "*Reverse Water Gas Shift*" (RWGS) (Davies and Lihou, 1971):

$$\begin{aligned} CO + 2H_2 &\rightleftarrows CH_3OH \\ CO_{2(g)} + 3H_{2(g)} &\rightleftarrows CH_3OH + H_2O_{(g)} \\ CO_2 + H_2 &\rightleftarrows CO + H_2O \end{aligned} \quad (15)$$

The kinetics of each one of the reactions can be computed following a simplified Langmuir-Hinshelwood model (Seidel et al., 2018). The catalyst is $Cu/ZnO/Al_2O_3$ and for it the rates, r_i, are given by eq. (16) as a function of the partial pressures of the species, p_i, the surface coverage, θ, and the oxidized centres, φ:

$$r_{CO} = (1-\phi)\cdot k_1 \cdot p_{CO} \cdot p_{H_2}^2 \left(1 - \left(\frac{p_{CH_3OH}}{K_{p1} p_{CO} \cdot p_{H_2}^2}\right)\right) \theta \cdot \theta^{x4}$$
$$r_{CO_2} = \phi^2 \cdot k_2 \cdot p_{CO_2} \cdot p_{H_2}^2 \left(1 - \left(\frac{p_{CH_3OH} p_{H_2O}}{K_{p2} p_{CO_2} \cdot p_{H_2}^3}\right)\right) \theta^{*2} \theta^{x4} \quad (16)$$
$$r_{RWGS} = \phi \cdot (1-\phi)^{-1} \cdot k_3 \cdot p_{CO_2} \left(1 - \left(\frac{p_{CO} p_{H_2O}}{K_{p3} p_{CO_2} \cdot p_{H_2}}\right)\right) \theta^{*2} \theta \cdot$$

Where ϕ represents the total amount of oxidised centres and 1- ϕ the number of reduced centres computed as follows:

$$\phi = 0.5\left(1-\left(\frac{1-\sqrt{K_1K_2\left(\frac{p_{CO}p_{H_2}}{p_{CO_2}\cdot p_{H_2O}}\right)}}{1+\sqrt{K_1K_2\left(\frac{p_{CO}p_{H_2}}{p_{CO_2}\cdot p_{H_2O}}\right)}}\right)\right) \quad (17)$$

The equilibrium constants K_1 and K_2 are given by eq. (18):

$$K_i = e^{\left(-\frac{\Delta G_i}{RT}\right)}$$
$$\Delta G_1 = 11.348\frac{kJ}{mol} \quad (18)$$
$$\Delta G_2 = 7.693\frac{kJ}{mol}$$

and the kinetic constants, k for each one of the reactions i are given by eq. (19), (Seidel et al., 2018):

$$k_1 = e^{\left(-4.7636+26.1883\left(\frac{523.15}{T}-1\right)\right)}$$
$$k_2 = e^{\left(-3.4112+3.4470\left(\frac{523.15}{T}-1\right)\right)} \quad (19)$$
$$k_3 = e^{\left(-5.7239+23.44744\left(\frac{523.15}{T}-1\right)\right)}$$

In addition, the equilibrium constants, K_p, are computed using the correlations presented in eq. (20), (Panahi et al., 2012; Graaf et al., 1986):

$$K_{p1} = 10^{\frac{5139}{T}-12.621}$$
$$K_{p2} = 10^{\frac{3066}{T}-10.592} \quad (20)$$
$$K_{p2} = 10^{-\frac{2073}{T}+2.029}$$

Variables $\theta^{\cdot}$, θ^{x} and θ^{*} correspond to the surface coverage of the catalyst as follows, eq. (21):

$$\theta^{\cdot} = \left(1+\beta_{11}\cdot p_{CO}+\beta_{12}\cdot p_{CH_3OH}+\beta_{14}\cdot p_{CO_2}\right)^{-1}$$
$$\theta^{x} = \left(1+\beta_7\sqrt{p_{H_2}}\right)^{-1} \quad (21)$$
$$\theta^{*} = \left(1+\beta_9\beta_{10}\frac{p_{H_2O}}{\beta_7^2 p_{H_2}}+\beta_{13}\cdot p_{CO_2}+\beta_8\cdot p_{CH_3OH}+\beta_9\cdot p_{H_2O}\right)^{-1}$$

Where p_i represents the partial pressure of each one of the species. It is assumed that the fugacity coefficients are close to 1. Table 2 shows the values for the β constants.

The pressure drop across the bed is computed using Ergun's equation as in the previous case where the values for the catalysis of the production of methanol are given in Table 3.

Table 2 – Values of the β constants (Seidel et al., 2018).

Constant	Value	Units
β_7	1.1665	$bar^{-0.5}$
β_8	0	bar^{-1}
β_9	0.0297	bar^{-1}
β_{10}	1600	bar^{-1}
β_{11}	0.147	–
β_{12}	0	bar^{-1}
β_{13}	0.04712	bar^{-1}
β_{14}	0	bar^{-1}

Table 3 – Characteristics of the catalyst for methanol production (Lücking, 2017).

Symbol	Parameters	Value	Units
ε	Porosity	0.285	–
μ	Viscosity	Variable	Pa·s
ρ	Density	Variable	kg/m^3
φ_σ	Shape factor	0.77	–
D_p	Particle diameter	0.0054	m
GG	Superficial mass flow	Variable	kg/m^2 s

Note that in this case the kinetics is given by the catalyst weight. Therefore, Ergun's equation is written as follows, eq. (22):

$$\frac{dP}{dW} = -\frac{G}{A_{tube}\rho_b\rho_o(\phi_\sigma D_p)\varepsilon^3}\left[\frac{150(1-\varepsilon)\mu}{\phi_\sigma D_p}+1.752G\right]\left(\frac{Pa}{kgcat}\right) \quad (22)$$

Where A_{tube} is the cross-sectional area of the reactor and ρ_b the apparent density of the catalyst, 1190 kg/m^3 (Lücking, 2017). The energy balance to the reactor bed is also reformulated as a function of the weight of catalysis (Fogler, 2001):

$$\frac{dT}{dW} = \frac{\sum_i(-r_i)\left[\Delta H_{R,i}(T_R)+\int_{T_R}^{T}\Delta C_p dT\right]}{F_{Ao}\left(\sum_{i=1}^{n}\Theta_i C_{p_i}+x\Delta C_p\right)} \quad (23)$$

where r_i is the kinetic rate of reaction i, ΔH_{R_i} its enthalpy of reaction, F_i the molar Flow of species i and C_{p_i} its heat capacity. The species balances are presented below, eq. (24):

$$\frac{dF_{CO}}{dW} = -r_{CO}+r_{RWGS}$$
$$\frac{dF_{H_2}}{dW} = -2\cdot r_{CO}-3\cdot r_{CO_2}-r_{RWGS}$$
$$\frac{dF_{CH_3OH}}{dW} = r_{CO}+r_{CO_2} \quad (24)$$
$$\frac{dF_{H_2O}}{dW} = r_{CO_2}+r_{RWGS}$$
$$\frac{dF_{CO_2}}{dW} = -r_{CO_2}-r_{RWGS}$$

2.3. *Optimization procedure*

The design of each of the reactors involves the selection of integer variables such as the number of beds, together with continuous variables related to the length or weight of each of the beds as well as the inlet temperature, pressure, and feedstock composition. A two-stage design procedure is followed. The effect of the pressure is analysed first by a sensitivity

analysis. In a second stage the reactor configuration and the operating conditions of the beds are obtained. As presented above, the complex kinetics involved in the reactions include highly nonlinear terms, while the optimization of the number of beds requires using integer decision variables. To ensure that a global minimum is found and to deal with the integer variables, a genetic algorithm approach for the mathematical optimization is proposed. In particular, the "ga" function in MATLAB has been selected for the task because of its capabilities for solving these kinds of problems by generating a population of solutions, scoring them, selecting the best performing individuals, and generating the next population by a crossover and mutation procedure. This function is used to optimize the operation of reactors that are involved in previous processes studied by Curto and Martín (2019) and Martin (2016b).

The objective function used in the genetic algorithm optimization represents the difference between the profit derived from selling the products and the annualized costs of equipment, cooling water, hydrogen fed and compression costs, eq. (25)

$$Z = C_{Prod} \cdot f_{prod} - C_W \cdot f_{Wa} - EC_{Anual} - C_{H_2} \cdot f_{H_2} - C_{Compression} \cdot W \quad (25)$$

Where the annualized cost of equipment is evaluated including the heat exchangers (HX), the shell (Shell) and the catalyst bed (Cat) as follows:

$$EC_{Anual} = \frac{1}{3}\left(C_{HX} + C_{Shell} + C_{Cat}\right) \quad (26)$$

The heat exchanger cost is taken from Almena and Martín (2016) as a function of the area, A, that is computed using the design equation for heat exchangers, eq. (27):

$$Q = U \cdot A \cdot LMTD \quad (27)$$

With the global heat transfer coefficient, U, equal to 200 ($W/m^2\,{}^{o}C$) (Brannan, 2002), and the logarithmic mean temperature difference, LMTD

$$HX \begin{cases} A < 25m^2 : HX = 39.59 \cdot (A(m^2))^{1.4915} \\ 25 < A < 140m^2 : HX = 1593.8(A(m^2)) + 2584.2 \\ A > 140m^2 : HX = 22.234 \cdot (A(m^2))^{0.4871} \end{cases} \quad (28)$$

The shell is assumed to be a vessel whose cost is assumed to be given by eqs. (29)–(30), Almena and Martín (2016):

$$Shell = W_{shell} \cdot C_{steel} \quad (29)$$

$$W_{Shell} = \rho_{steel}\left(\pi\left[\left(\frac{D_c}{2} + e\right)^2 - \left(\frac{D_c}{2}\right)^2\right]L + \frac{4}{3}\pi\left[\left(\frac{D_c}{2} + e\right)^3 - \left(\frac{D_c}{2}\right)^3\right]\right) \quad (30)$$

Where C_{steel} represents the cost of stainless steel and has a value of 2.4 €/kg (MEPS, 2020), ρ_{steel}, the density of stainless steel is 7850 kg/m^3, D_c is the inner diameter of the cylinder and e is the thickness of the shell walls, which is calculated as follows:

$$e(in) = \frac{P \cdot R}{S \cdot E - 0.6 \cdot P} \quad (31)$$

Where S has a value of 21,000 psi and E, a value of 0.9. P is the operating pressure in psi.

The cooling water cost has a value of 2 €/m^3 (INE, 2006).

The methanol catalyst costs 113.2 €/kg (ALFA AESAR, 2020) while the methane catalyst costs 500 €/kg (El-Sibai, 2019). Two prices for hydrogen are used, 0 €/kg and 4 €/kg, to present the range of prices up to the one of renewable based hydrogen (www.spglobal.com). The compression costs are included considering an electricity cost of 0.08 €/kWh (REE, 2020).

Two reactors are evaluated, first the biomethanation reactor where the CO_2 within the biogas is hydrogenated using renewable hydrogen. In this case, the feed ratio is given by eq. (32).

$$b = \frac{H_2}{CO_2} \quad (32)$$

And the range of the operating variables considered is b from 0.5 to 5, total pressure of 15 atm or 20 atm, with each reactor bed length limited by an upper bound of 0.3 m and up to 6 beds are considered. Different maximum temperatures after each bed are considered, 700 K, 750 K and 800 K.

In the case of the production of methanol, two different feed ratios are defined by eq. (33):

$$a = \frac{H_2}{CO} \qquad d = \frac{H_2 - CO_2}{CO - CO_2} \quad (33)$$

Where the range of values for a is from 1.5 to 3, d ranges from 1.5 to 2.5. The operating pressures of 50 and 100 atm are evaluated and up to 8 beds. To produce methanol, only CO_2 and H_2 are eventually fed, and d ratio becomes b defined by eq. (32).

3. Results

The presentation of the results separates both cases of study. First, the results of the design of the biogas methanation reactor are presented. Next, the methanol production unit results are shown and discussed.

3.1. *Biomethane reactor*

The feed to the reactor is at 600 K (Martín, 2016a) while the biogas composition (CO_2: 46.01; H_2: 365.4; CH_4: 103.725 kmol/h) is taken from the literature (Martín et al., 2018) where a facillty to process 10 kg/s of waste at industrial scale was considered. The first stage evaluates the effect of the operating pressure, considering the typical upper limit from the literature (Falbo et al., 2018; Schlereth and Hinrchsen, 2014). Fig. 2 shows that the feed pressure has a negligible effect on the profit. Apart from the effect of the pressure, the larger the hydrogen ratio in the feed, the larger the production of methane that is to be expected. The cost of hydrogen and its renewable production is the main limitation.

Since the effect of the pressure is small, the lowest value, 15 atm, is selected. Next, the design of the reactor configuration, number of beds, and operating variables, feed temperature and gas composition, beds lengths, as well as the maximum

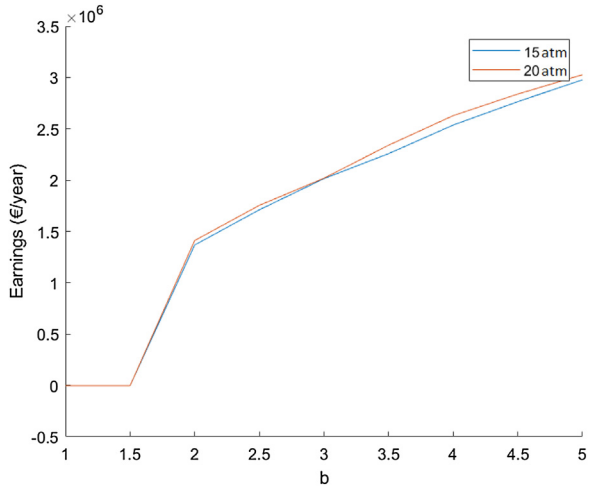

Fig. 2 – Effect of the pressure on the profit.

ΔT across each bed (ΔT_{max}), are optimized. Two prices of hyrogen are evaluated, 0 €/kg and 4 €/kg.

The best reactor configuration depends on the hydrogen cost and the maximun ΔT allowed across a single bed. Reasonable values for that ΔT_{max} are assumed to be 100 K, 150 K and 200 K. For these three values, Fig. 3 shows the optimal profile of the different species along the beds. As the ΔT_{max} allowed is larger, the number of beds required decreases abruptly. For hydrogen at no cost, the number of beds goes from 5, for ΔT_{max} equal to 100 K, to 2 in the rest of the cases. Previous studies used three beds (Mancusi et al., 2021) or five beds (Tripodi et al., 2020) with no previous methane in the feedstock which allowed high conversions of hydrogen. Four beds were used at lab scale to hydrogenate biogas reaching 90% conversion of CO_2 using a b ratio equal to 4 but no results where reported on temperature profiles across each bed (Gaikwad et al., 2020). Another interesting insight is that the number of beds is smaller for a higher cost of hydrogen, 4 €/kg, the one corresponding to renewable hydrogen. Thus, the number of beds is 2 for ΔT_{max} equal to 100 K, only one bed is recommended in the other two cases. In addition, the feed ratio b,

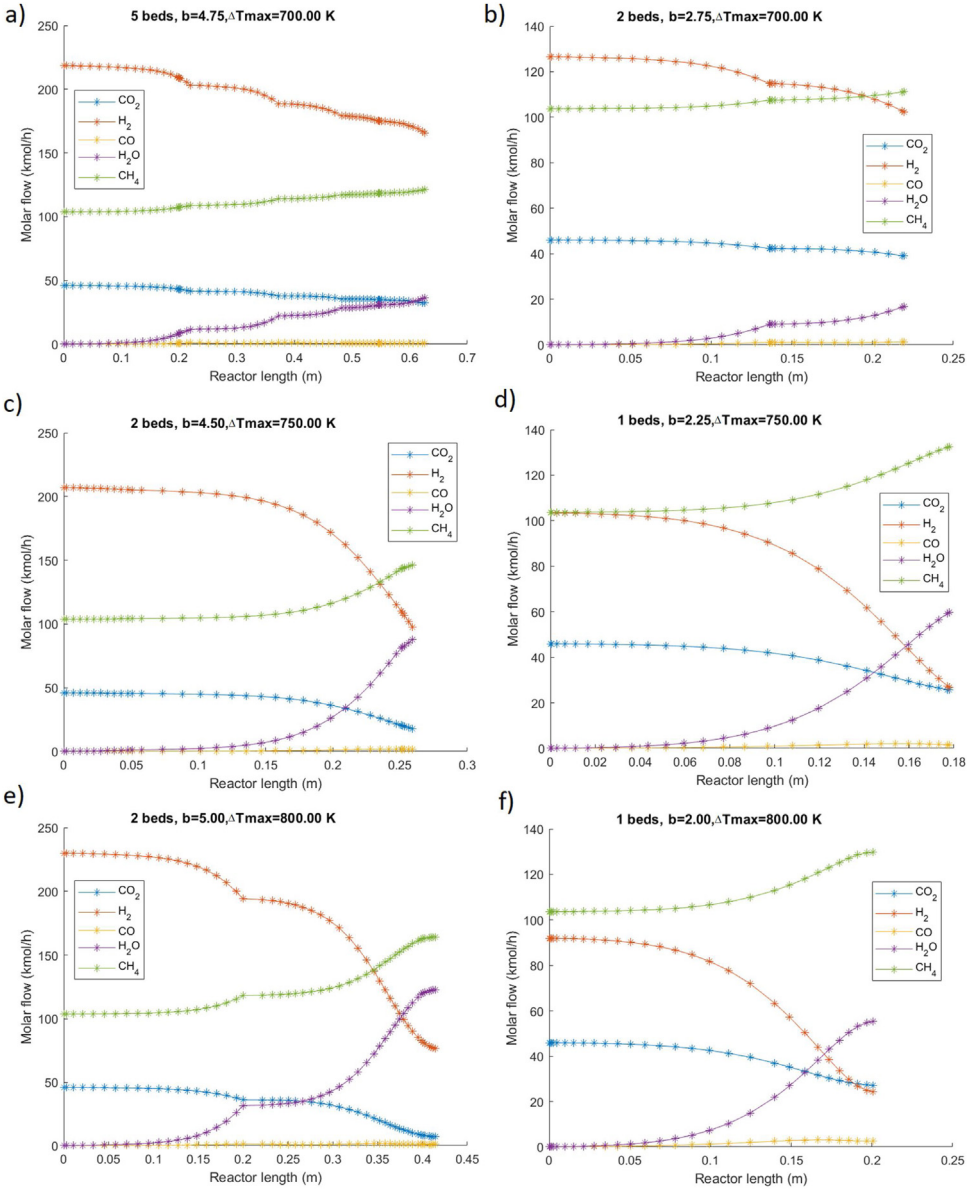

Fig. 3 – Concentration profiles along the multibed reactor: a) ΔT_{max} = 700 K, P_{H2} = 0 €/kg; b) ΔT_{max} = 700 K, P_{H2} = 4 €/kg; c) ΔT_{max} = 750 K, P_{H2} = 0 €/kg; d) ΔT_{max} = 750 K, P_{H2} = 4 €/kg; & e) ΔT_{max} = 800 K, P_{H2} = 0 €/kg; f) ΔT_{max} = 800 K, P_{H2} = 4€/kg.

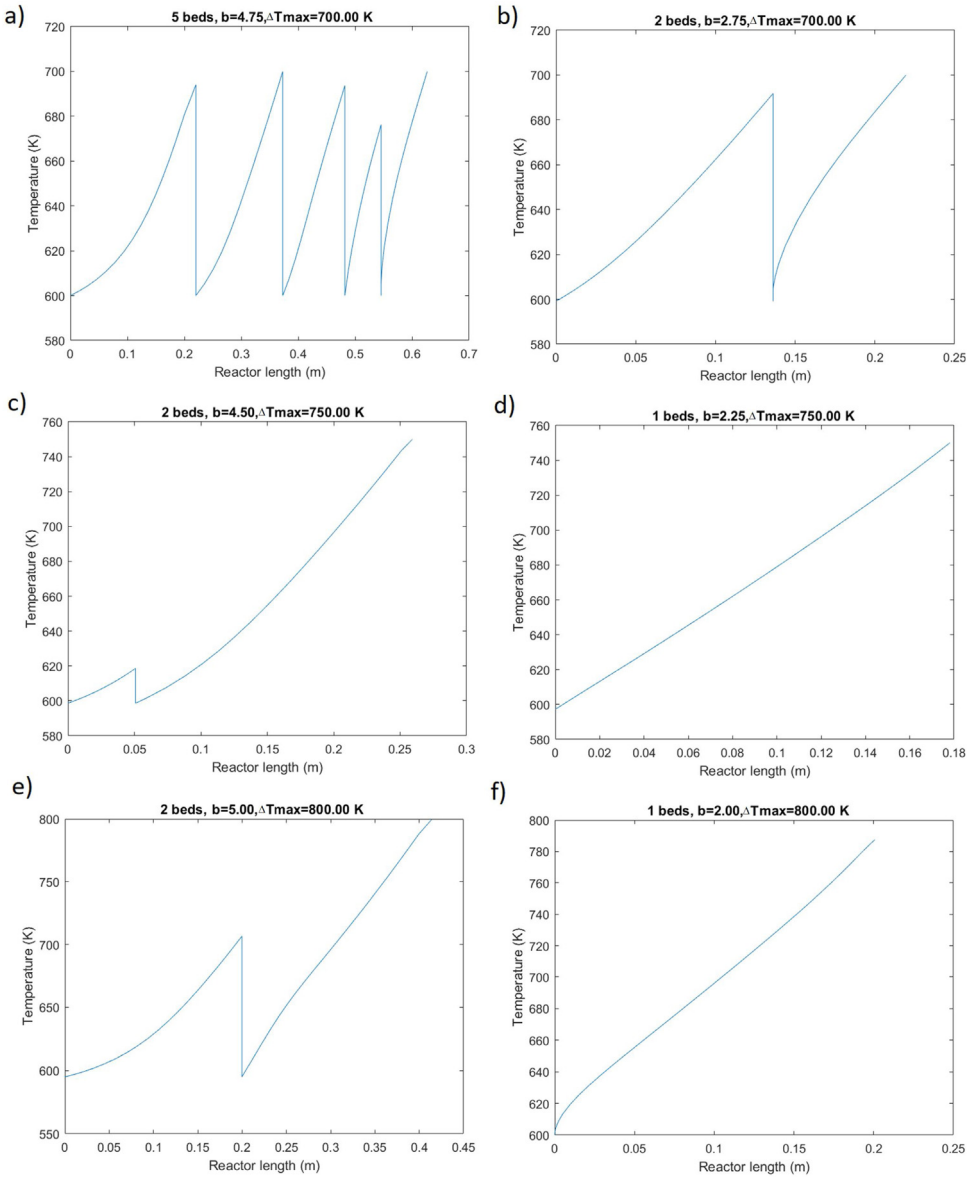

Fig. 4 – Temperature profiles along the multibed reactor: a) ΔT_{max} = 700 K, P_{H2} = 0 €/kg; b) ΔT_{max} = 700 K, P_{H2} = 4 €/kg; c) ΔT_{max} = 750 K, P_{H2} = 0 €/kg; d) ΔT_{max} = 750 K, P_{H2} = 4 €/kg; & e) ΔT_{max} = 800 K, P_{H2} = 0 €/kg; f) ΔT_{max} = 800 K, P_{H2} = 4 €/kg.

representing the mount of hydrogen fed to the system, is not recommended to reach the upper bound but in the case of free hydrogen and the higher value of ΔT_{max}, 200 K. For the case of hydrogen at 4 €/kg, b takes values around half the ones compared to the ones obtained a zero cost, from 2.75 to 2, instead of values around 5-4.5, as the ΔT_{max} across the bed increases from 100 K to 200 K. The conversion across the reactor increases with ΔT_{max}, as expected. For lower ΔT_{max} allowed across the catalytic bed, the conversion increases step by step as the fluid advances from one bed to the next. However, as ΔT_{max} is allowed to be equal to or above 150 K, most of the coversion is achieved in the second bed. Fig. 4 shows the temperature profile along the different reactor beds. When the solution shows more than 1 bed, ΔT across the first bed is always below 100 K, even if it is allowed to be larger, justifying the larger conversion achieved from the second bed onwards. To avoid hot spots ΔT_{max} equal to 100 K is considered as the best case. It is reported in the literature that in 20 cm the temperature is peaked (Dannesboe et al., 2020) showing similar bed lengths as the ones presented in Fig. 3. In addition, the b ratios recommended in the same work are closer to the ones found when hdyrogen can be obtained for free, as well as the ones presented in Falbo et al. (2018), which shows the importance of the optimization to select the operating conditions.

3.2. *Methanol reactor*

In the production of methanol there is an entire trend towards working at pressures around 50 atm, known as LTMEOH (Martín, 2016a; Kiss et al., 2016), due to the high cost derived from operating at higher pressure. The analysis and optimization of the methanol synthesis reactor is carried out following a two-stage procedure. In the first stage, the pressure and the two feed ratios are evaluated, and the results are presented for several scenarios. Next, with the pressure, and a feed consisting of H_2 and CO_2, the reactor configuration and operating conditions are optimized.

Fig. 5 shows the results of the first stage, presenting the effect of the feed composition and the pressure in the profit. If the compression cost of the feed is not considered, it is preferable to operate at 100 atm, like the results presented by Kiss et al. (2016), and low values of ratio a are suggested, while the effect of the feed ratio defined by b is small. The difference in earnings per year between both

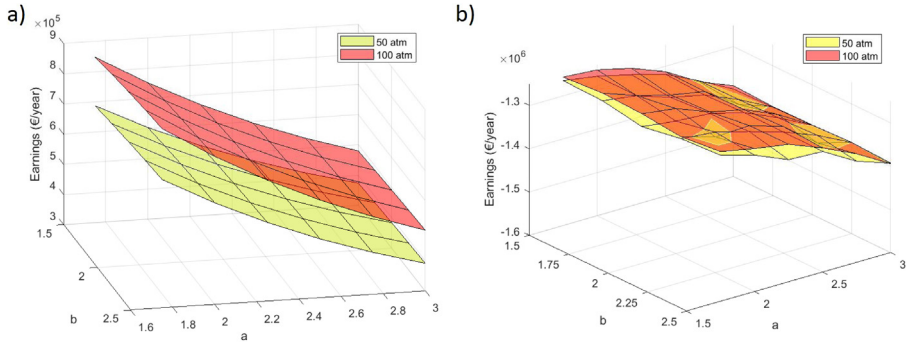

Fig. 5 – Effect of pressure and feed composition in the profit for methanol production. a) 0 €/kg of H_2; b) 4 €/kg of H_2.

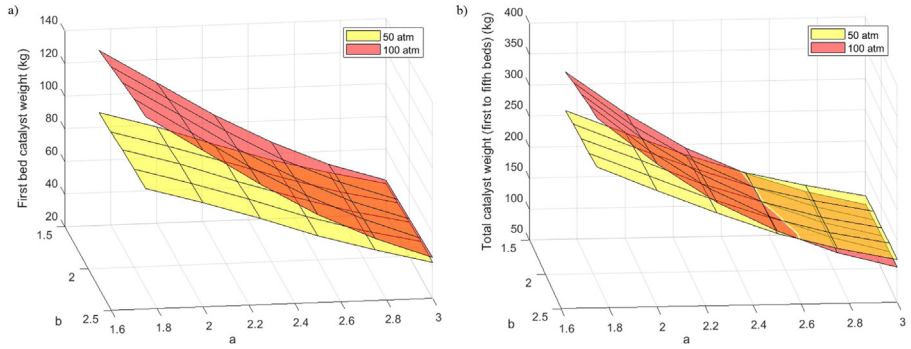

Fig. 6 – Effect of presure on the bed length. a) First bed: b) Total of the fifth first beds. 0 €/kg Cost of H_2.

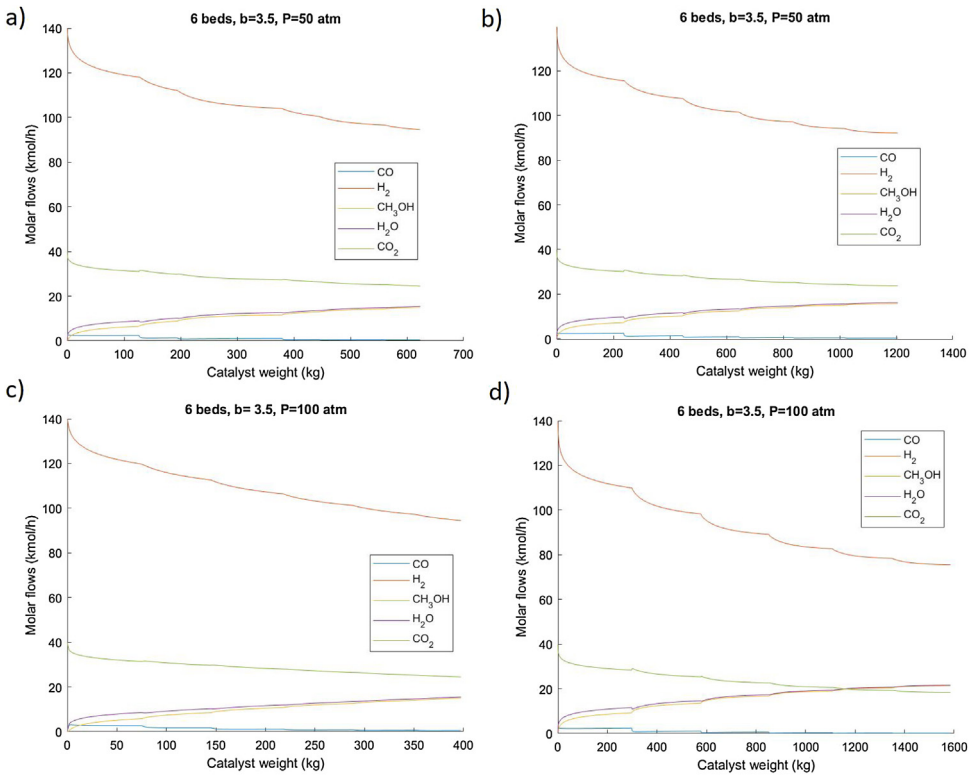

Fig. 7 – Concentration profiles along the beds in methanol production a) 4 €/kg Cost, 50 atm; b) 0 €/kg, Cost 50 atm; d) 4 €/kg, 100 atm d) 0 €/kg, 100 atm.

cases is in the order of 200.000 €/year. Taking into account the cost of compression for a 100 kmol/h stream, considering an electricity cost of 0.08 €/kWh, plus the cost of a higher pressure equipment in the plant, the operating cost goes up to 10^6 €/year, so that the improvement in the yield to methanol due to the higher pressures does not mitigate the additional costs.

The length of the bed required is shorter the larger the concentration of hydrogen in the feed and the lower the operating pressure. An example for the first bed is presented in Fig. 6. The total mass of catalyst used is similar for both pressures, it decreases with the concentration of H_2 and it is barely affected by b ratio. The feed ratios b and a turned out to be 2.5 and 1.75 respectively under any pressure.

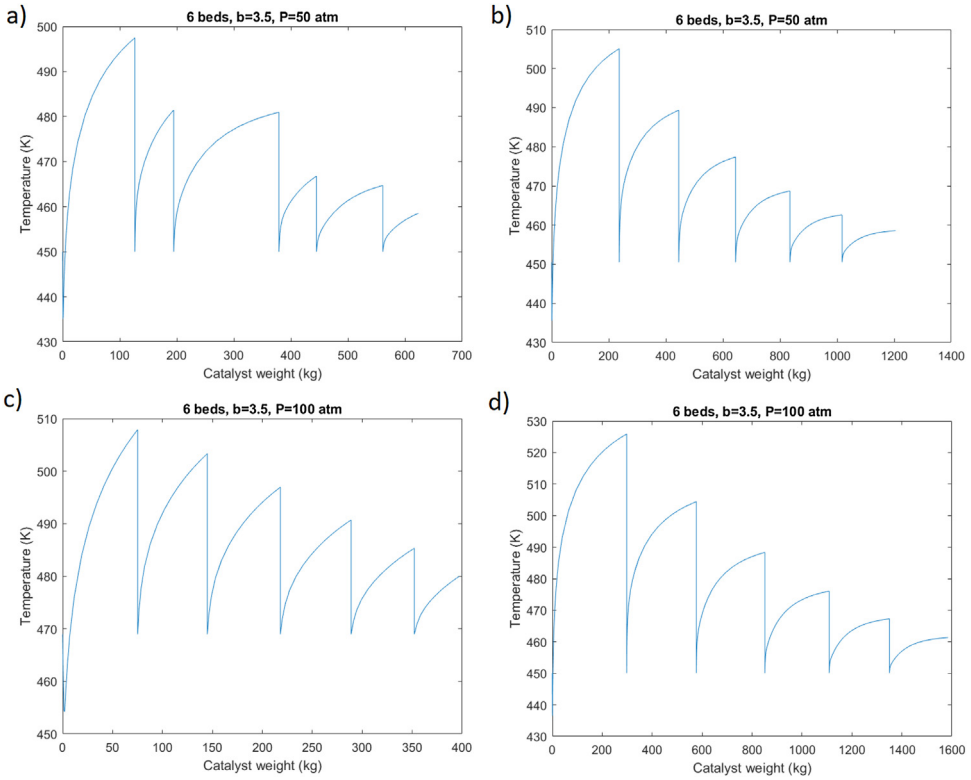

Fig. 8 – Temperature profiles along the reactor beds for methanol production. a) 4 €/kg Cost, 50 atm; b) 0 €/kg, Cost 50 atm; d) 4 €/kg, 100 atm d) 0 €/kg, 100 atm.

To produce methanol from CO_2 hydrogenation, the operating conditions are optimized for two prices of hydrogen. Even though working at 50 atm is favoured (Gallucci et al., 2004), results for 50 atm and 100 atm are presented, the same range as in Kiss et al. (2016). For the feed conditions an upper bound for the ratio H_2 to CO_2 is fixed to 3.5, considering the results shown above, the fact that Rafiee (2020) recommend a value of 3, as well as Gallucci et al. (2004), while Kiss et al. (2016) and Gallucci et al. (2004) showed improvement for ratios above that, b defined as per eq. (31), which is equivalent to a d given by eq. (32) equal to 2.5 if no CO is fed. The decision variables are the number of beds and their length. The number of beds turns out to be 6 at any of the two operating pressures and hydrogen costs, see Fig. 7, while some previous studies show the use of either 1 bed or 6 beds with water separation (Leonzio et al., 2019). For a price of hydrogen of 4 €/kg, a minimum production of methanol was imposed since the profit was negative. The effect of the cost of H_2 does not affect the configuration of the reactor. In addition, the optimization leads to reduce the use of the catalyst by half achieving the same methanol production capacity. Another interesting result is that at 50 atm, when hydrogen is fed at no cost, the size of the different beds is not the same, maybe because it is limiting the performance. The fractional conversion is the largest at the first bed and decreases with the number of beds, but it is always significant. The ΔT at each bed is around 100 K at the most, see Fig. 8, that takes place along the first reactor bed where the largest fractional conversion is achieved, and it decreases bed after bed. The relatively low cost of the catalyst does not suggest a fewer number of beds. The profile of the operation of the reactor is presented in Fig. 9 using up to 8 beds. We see that last two beds only provide an additional 5% conversion and thus the selected number of beds is 6. Compared to the previous case, this reaction is not that exothermic and the conversion

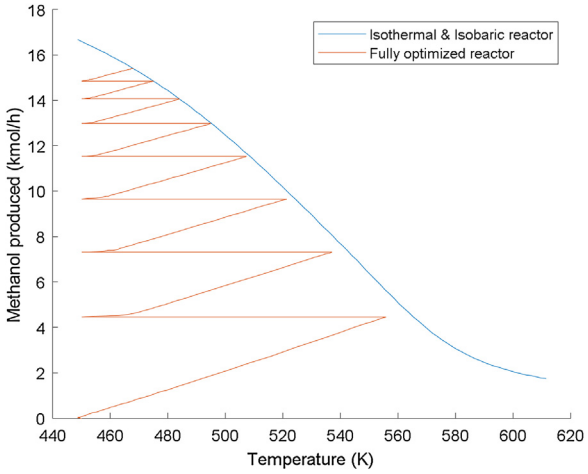

Fig. 9 – Methanol production profile across the beds.

by step is smaller, which results in a larger number of beds suggested.

4. Conclusions

In this work a genetic algorithm has been used for the optimal design of CO_2 hydrogenation reactors, either to produce biomethane via biogas-based CO_2 hydrogenation or the production of methanol from captured CO_2. Detailed kinetics for the multibed reactors is used defining the operating conditions such as inlet temperature, temperature profile, pressure, feed composition and number of beds. The evaluation of the entire reactor provides further insight compared to previous studies focused on the kinetics or on the operation of a single bed. Considering that the hydrogen costs represent a high share of the production costs of any hydrogenated based prod-

uct, a comparison between the optimal reactor configurations for different hydrogen costs and feed conditions is provided.

In the case of the methanation of the CO_2 of the biogas, the optimal reactor configuration suggests 2 beds to avoid sinterization due to excessive ΔT across the catalytic beds. The optimal b ratio is equal to 2.75 and an operating pressure of 15 atm is suggested. The reaction yield increases substantially if ΔT_{max} across the bed is allowed above 100 K, reducing the need for hydrogen in the feed to a b ratio of 2. If the hydrogen comes for free, the number of beds and the fraction of hydrogen in the feed increases to 5 and 4.75 respectively.

In the case of methanol production via CO_2 hydrogenation, the optimal operating temperature results in 50 atm, in accordance with current trend to reduce power consumption in the operation of the process. It was found that the improvement in methanol production by using high pressure conditions (100 atm) instead of low pressure (50 atm), does not compensate for the higher equipment and operational costs associated with it. The feed ratio of hydrogen to CO_2 turned out to be 3.5 and a 6-bed reactor is the suggested configuration.

Declaration of interests

The authors declare that they have no known competing financial interests or personal relationships that could have appeared to influence the work reported in this paper.

Data availability

The data that has been used is in the cited papers and reports.

Acknowledgments

Authors thank University of Salamanca GIR PSEM3 group for software licenses and Junta de Castilla y León project SA026G18.

References

ALFA AESAR, 2020. 45776 Copper based methanol synthesis catalyst. https://www.alfa.com/en/catalog/045776/. Last accessed April 2020.

Almena, A., Martín, M., 2016. Techno-economic analysis of the production of epichlorohydrin from glycerol. Ind. Eng. Chem. Res. 55, 3226–3238.

Anicic, B., Trop, P., Goricanec, D., 2014. Comparison between two methods of methanol production from carbon dioxide. Energy 77, 279–289.

Bader, A., Bauersfeld, S., Brunhuber, C., Pardemann, R., Meyer, B., 2011. Modelling of a chemical reactor for simulation of a methanisation plant. In: Presentation 063:064. Proceedings of the 8th International Modelica Conference, March 20th-22nd, Technical University, Dresden, Germany 2011 https://modelica.org/events/modelica2011/Proceedings/pages/papers/44_4_ID_202_a_fv.pdf.

Borisut, P., Nuchitprasittichai, A., 2019. Methanol production via CO2 hydrogenation: sensitivity analysis and simulation—based optimization. Front. Energy Res. 7, 81, http://dx.doi.org/10.3389/fenrg.2019.00081.

Brannan, C.R., 2002. Rules of Thumb for Chemical Engineers. McGraw Hill, New York.

Cuéllar-Franca, R.M., Azapagic, A., 2015. Carbon capture, storage and utilisation technologies: a critical analysis and comparison of their life cycle environmental impacts. J. CO2 Utilization 9, 82–102.

Curto, D., Martín, M., 2019. Renewable based biogas upgrading. J. Clean. Prod. 224, 50–59.

Dannesboe, C., Hansen, J.B., Johannsen, I., 2020. Catalytic methanation of CO2 in biogas: experimental results from a reactor at full scale. React. Chem. Eng. 5, 183–189.

Davies, J., Lihou, D., 1971. Optimal design of methane steam reformer. Int. J. Chem. Process. Eng. Res. 52, 71–80.

Davis, W., Martín, M., 2014a. Optimal year-round operation for methane production from CO_2 and water using wind energy. Energy 69, 497–505.

Davis, W., Martín, M., 2014b. Optimal year-round operation for methane production from CO_2 and water using wind and/or solar energy. J. Clean. Prod. 80, 252–261.

de la Cruz, V., Martin, M., 2016. Turbine characterization selection and optimal design under uncertainty. J. Clean. Prod. 133, 1302–1311.

El-Sibai, A., 2019. Model-Based Optimization and Experimental Investigation of CO2 Methanation. PhD Thesis. Otto-von-Guericke-Universität Magdeburg 2019, http://dx.doi.org/10.25673/32608.

Fache, A., Marias, F., Guerré, V., Palmade, S., 2018. Optimization of fixed-bed methanation reactors: safe and efficient operation under transient and steady-state conditions. Chem. Eng. Sci. 192, 1124–1137.

Falbo, L., Martinelli, M., Visconti, C., Lieti, L., Bassano, C., Deiana, P., 2018. Kinetics of Co2 methanation on a Ru-based catalyst at process conditions relevant to power-to-gas applications. Appl. Catal. B: Environ. 225, 354–363.

Fogler, H.S., 2001. Elements of Chemical Reactor Engineering. Prentice-Hall Inc., New Jersey.

Gaikwad, R., Villadsen, S.N.B., Rasmussen, J.P., Grumsen, F.B., Nielsem, L.P., Gildert, G., Moller, P., Fosbol, P.L., 2020. Container-sized CO_2 to methane: design, construction and catalytic tests using raw biogas to biomethane. Catalysts 10, 1428.

Gallucci, F., Paturzo, L., Basile, A., 2004. An experimental study of CO_2 hydrogenation into methanol involving a zeolite membrane reactor. Chem. Eng. Process. Proc Int. 43 (8), 1029–1036.

Gassner, M., Marechal, F., 2009. Thermo-economic process model for thermochemical production of Synthetic Natural Gas (SNG) from lignocellulosic biomass. Biomass Bioener. 33, 1587–1604.

Graaf, G.H., Sijtsema, P.J.J.M., Stamhuis, E.J., Joosten, G.E.H., 1986. Chemical equilibria in methanol synthesis. Chem. Eng. Sci. 41, 2883–2890.

Gunaseelan, V.N., 1997. Anaerobic digestion of biomass for methane production: a review. Biomass Bioener. 13 (12), 83–114.

Hernández, B., Martín, M., 2016. Optimal process operation for biogas reforming to methanol: effects of dry reforming and biogas composition. Ind. Eng. Chem. Res. 55 (23), 6677–6685.

Hwang, S., Smith, S., 2008. Heterogeneous catalytic reactor design with non-uniform catalyst considering shell-progressive poisoning behavior. Chem. Eng. Technol. 31 (3), 384–397.

INE, In Spanish 2006. National statistics institute. Water indicators Indicadores sobre el agua. https://www.ine.es/jaxi/Datos.htm?path=/t26/p069/p03/serie/l0/&file=01003.px#!tabs-tabla.

Kirchbacher, F., Miltner, M., Lehner, M., Steinmuller, H., Harasek, M., 2016. Demonstration of a biogas methanation combined with membrane based gas upgrading in a promising power-to-gas concept. Chem. Eng. Trans. 52, 1231–1236.

Kiss, A.A., Pragt, J.J., Vos, H.J., Bargeman, G., De Groot, M.T., 2016. Novel efficient process for methanol synthesis by CO_2 hydrogenation. Chem. Eng. J. 284, 260–269.

Korhonen, J., Honkasalo, A., Seppala, J., 2018. Circular economy: the concept and its limitations. Ecol. Econ. 143, 37–46.

Leonzio, G., Zondervan, E., Foscolo, P.U., 2019. Methanol production by CO_2 hydrogenation: analysis and simulation of reactor performance. Int. J. Hydrogen Energy 44 (16), 7915–7933.

Lücking, L., 2017. Methanol Production From Syngas. Delft University of Technology, pp. 113.

Mancusi, E., Bareschino, P., Forgione, A., Tregambi, G., Pepe, F., 2021. CO_2 methanation: reactor modelling and parametric análisis. Comp. Aided. Chem. Eng. 50, 585–590.
Martin, M., 2016b. Methodology for solar and wind based process design under uncertainty: methanol production from CO_2 and hydrogen. Comp. Chem. Eng. 92, 43–54.
Martín, M., 2016a. Industrial Chemical Process Analysis and Design. Elsevier, Oxford, UK.
Martín, E., Sampat, A., Martín, M., Zavala, V., 2018. Optimal integrated facility for waste processing. Chem. Eng. Res. Des. 131, 160–182.
Materazzi, M., Grimaldi, F., Foscolo, P.U., Cozens, P., Taylor, R., Chapman, C., 2017. Analysis of syngas methanation for bio-SNG production from wastes: kinetic model development and pilot scale validation. Fuel Process. Technol. 167, 292–305.
MEPS 2020. Europe steel prices. https://www.meps.co.uk/gb/en/products/europe-steel-prices. Last accessed 15 March 2020.
Meyer, J.J., Tan, P., Apfelbacher, A., Daschner, R., Hornung, A., 2016. Modeling of a methanol synthesis reactor for storage of renewable energy and conversion of CO_2 – comparison of two kinetic models. Chem. Eng. Technol. 39 (2), 233–245.
Milani, D., Khalilpour, R., Zahedi, G., Abbas, A., 2015. A model-based analysis of CO_2 utilization in methanol synthesis plant. J. CO2 Utilization 10, 12–22.
Panahi, P.N., Mousavi, S.M., Niaei, A., Farzi, A., Salari, D., 2012. Simulation of methanol synthesis from synthesis gas in fixed bed catalytic reactor using mathematical modeling and neural networks. Int. J. Sci. Eng. Res. 3 (2), 1–7.
Pérez-Fortes, M., Schoneberger, J.C., Boulamanti, A., Tzimas, E., 2016. Methanol synthesis using captured CO_2 as raw material: techno-economic and environmental assessment. Appl. Energy 161, 718–732.
Rafiee, A., 2020. Modelling and optimization of methanol synthesis from hydrogen and CO_2. J. Environ. Chem. Eng. 8 (2020), 104314.
REE 2020 RED ELÉCTRICA DE ESPAÑA, 2020. Mercados y precios. Last seen 13 April 2020 https://www.esios.ree.es/es/mercados-y-precios.
Rönsch, S., Schneider, J., Matthischke, S., Schlüter, M., Götz, M., Lefebvre, J., Prabhakaran, P., Bajohr, S., 2016. Review on methanation-from fundamental to current projects. Fuel 166, 276–296.
Sahebdelfar, S., Ravanchi, M.T., 2015. Carbon dioxide utilization for methane production: a thermodynamic analysis. J. Petrol. Sci. Eng. 134, 14–22.
Sánchez, A., Martín, M., 2018. Optimal renewable production of ammonia from water and air. J. Clean. Prod. 178, 325–342.
Schaaf, T., Grunig, J., Schuster, M.R., Rothenflush, T., Orth, A., 2014. Methanation of CO_2 - storage of renewable energy in a gas distribution system. Energy Sust. Soc. 4, 2, http://dx.doi.org/10.1186/s13705-014-0029-1.
Schidhauer, T.J., Biollaz, S.M.A., 2015. Reactors for catalytic methanation in the conversion of biomass to synthetic natural gas (SNG). ThE SWISS COmpETEnCE CEnTER fOR EnERgy RESEaRCh On BIOEnERgy CHIMIA 2015 69 (10), 603–607.
Schlereth, D., Hinrchsen, O., 2014. A fixed-bed reactor modeling study on the methanation of CO_2. Chem. Eng. Res. Des. 92 (849), 702–712.
Seidel, C., Jörke, A., Vollbrecht, B., Seidel-Morgenstern, A., Kienle, A., 2018. Kinetic modeling of methanol synthesis from renewable resources. Chem. Eng. Sci. 175, 130–138.
Stangeland, K., Kalai, D., Li, H., Yu, Z., 2017. CO_2 methanation: the effect of catalyst and reaction conditions. Energy Procedia 105, 2022–2027.
Taifouris, M.R., Martín, M., 2018. Multiscale scheme for the optimal use of residues for the production of biogas across Castile and Leon. J. Clean. Prod. 185, 239–251.
Tripodi, A., Conte, F., Rossetti, I., 2020. Carbon dioxide methanation: design of a fully integrated plant. Energy Fuels 34 (86), 7242–7256.
Tynjala, T., 2015. Biological Methanation of Hydrogen: A Way to Increase Methane Yield in Biogas Plants 2015. http://www.neocarbonenergy.fi/wp-content/uploads/2016/02/06_Tynjala.pdf.
Uebbing, J., Rihko-Struckmann, L., Sager, S., Sundmacher, K., 2020. CO_2 methanation process synthesis by superstructure optimization. J. CO2 Utilization 40, 101228.
Van-Dal, E.S., Bouallou, C., 2013. Design and simulation of a methanol production plant from CO_2 hydrogenation. J. Clean. Prod. 57, 38–57.
Vara, G., 2000. Capítulo 4: Ingeniería de proyecto. Proyecto de Grado. http://www.contechs.org/Projecto%20de%20Grado%20de%20Gonzalo%20y%20Vara/CAPITULO%204.pdf.
Witte, J., Calbry-Muzyka, A., Wieseler, T., Hottinger, P., Biollaz, S.M.A., Schildhauer, T.J., 2010. Demonstrating direct methanantion of real biogas in a fluidized bed reactor. Appl. Energy 240, 359–371.
World Energy Council World Energy Resources Waste to Energy | 2016, https://www.worldenergy.org/wp-content/uploads/2017/03/WEResources_Waste_to_Energy_2016.pdf.
Xu, J.G., Froment, G.F., 1989. Methane steam reforming, methanation and water-gas shift: I. Intrinsic kinetics. AIChE J. 35, 88–96.
Zimmermann, R.T., Bremer, J., Sundmacher, K., 2020. Optimal catalyst particle design for flexible fixed-bed CO2 methanation reactors. Chem. Eng. J. 387, 123704, . Last accessed September 2021 https://www.spglobal.com/marketintelligence/en/news-insights/latest-news-headlines/experts-explain-why-green-hydrogen-costs-have-fallen-and-will-keep-falling-63037203.